GEOTECTONICS AND GEODYNAMICS

УДК 550.34+550.341
DOI: 10.46698/VNC.2022.92.93.005

Original paper

Monte Cristo Range earthquake May 15, 2020: calculated intensity and macroseismic field

O. O. Erteleva[1], F. F. Aptikaev[1], K. S. K. Karthik Reddy[2], S. Chanda[2], S. N. Somala[2]

[1]Schmidt Institute of Physics of the Earth of the Russian Academy of Sciences, 10/1 Bolshaya Gruzinskaya, Moscow 123242, Russian Federation, e-mail: ertel@ifz.ru;

[2]Indian Institute of Technology Hyderabad, 502285, India

Received: 10.02.2022, revised: 22.02.2022, accepted: 04.03.2022

Abstract: Relevance. When studying the seismic effect of the occurred earthquake, the collected macroseismic data are of great importance. To design the most reliable map of the macroseismic field, it's necessary to have the sufficient number of such data, which descript accurately, how and under what circumstances the earthquake was felt. However, in sparsely populated regions, collecting such information is often impossible. In similar situations, the lack of near-field data is particularly sensitive. This is the case of the Monte Cristo Range earthquake, 15.05.2020, M_W = 6.5, which occurred in Western Nevada. The nearest settlement from the epicenter was at a distance of» 59 km. In addition, there were not only strong ground motion instruments, but also regional seismic stations near the epicenter. The nearest seismic station that recorded the event was at a distance of» 39 km. In the absence of information or their extremely small number, the construction of isoseists near the epicenter can be made only by theoretical calculations. Global or regional empirical attenuation curve is used. Usually, the attenuation law is described by single curve. The accuracy of such constructions is low. The separation of several zones in the earthquake wave field with their individual attenuation laws and the correlations between the vibration parameters and the parameters of the earthquake source and ground conditions significantly improves the accuracy of calculations. The article proposes a methodology for calculating accelerations and intensities based on empirical data. **The aim of the work** is study of the macroseismic field of the Monte Cristo Range earthquake, 15.05.2020, M_W = 6.5: assessment of peak accelerations and intensity in the near-field of this earthquake. **Research methods** – analysis of available data on the earthquake, and development of attenuation curves for this seismic event, calculation of peak ground accelerations, duration of oscillations and assessing intensity. **Results of the work** – for Monte Cristo Range earthquake, 15.05.2020, PGA attenuation equations were proposed and the seismic effect in the near-field was estimated.

Keywords: seismic effect, epicenter, magnitude, peak ground acceleration, peak ground velocity, duration, intensity, macroseismic field.

Acknowledgements: *This work is partially funded by the Department of Science and Technology, India, INT/RUS/RFBR/P-335 and Ministry of Earth Sciences MoES/P. O (Seismo)/1 (304)/2016, and also was carried out under the state task of Schmidt Institute of Physics of the Earth, Russian Academy of Sciences, and was supported by the Russian Foundation for Basic Research (grant no. 18-55-45010 IND_a). The Nevada regional seismic network (NN) monitors earthquake activity throughout Nevada and many areas of Eastern California. The complete network includes about 450 channels of real-time waveform data collected from a variety of instrumentation. NN network data was accessed through IRISDMC. The Southern California Earthquake Data Center (SCEDC), funded by the Southern California Earthquake Center (SCEC) and other sources, holds the complete data archives for SCSN/CISN from 1932 to present. Southern California Seismic Network operated by Caltech and USGS were accessed through SCEDC. Waveform data, metadata, or data products for this study were accessed through the Northern California Earthquake Data Center. UC Berkeley contributed this data to the NCEDC.*

For citation: Erteleva O. O., Aptikaev F. F., Reddy Karthik K. S. K., Chanda S., Somala S. N. Monte Cristo Range earthquake May 15, 2020: calculated intensity and macroseismic field. *Geologiya I Geofizika Yuga Rossii = Geology and Geophysics of Russian South*. 2022. 12 (1): 62-74. DOI: 10.46698/VNC.2022.92.93.005.

ГЕОТЕКТОНИКА И ГЕОДИНАМИКА

DOI: 10.46698/VNC.2022.92.93.005

Оригинальная статья

Землетрясение Монте Кристо Рэйндж, 15 мая 2020 г.: расчетная интенсивность и макросейсмическое поле

О. О. Эртелева[1], Ф. Ф. Аптикаев[1], К. С. К. Картик Редди[2], С. Чанда[2], С. Н. Сомала[2]

[1]ФГБУН Институт физики Земли РАН им. О. Ю. Шмидта, Россия, 123242, Москва, ул. Большая Грузинская, 10, стр. 1, e-mail: ertel@ifz.ru;

[2]Индийский технологический институт, факультет гражданского строительства, Хайдерабад, 502285, Индия

Статья поступила: 10.02.2022, доработана: 22.02.2022, одобрена в печать: 04.03.2022

Резюме: Актуальность работы. При исследовании сейсмического эффекта происшедшего землетрясения большое значение имеют собранные макросейсмические данные. Их достаточное количество и точность описания того, как и при каких обстоятельствах ощущалось землетрясение, способствуют построению наиболее достоверной карты макросейсмического поля. Однако в малонаселенных регионах сбор такой информации зачастую невозможен. В подобных ситуациях особенно чувствителен недостаток данных в ближней зоне землетрясений. Именно такой случай представляет собой землетрясение Монте Кристо Рэйндж, 15.05.2020 г., M_W = 6,5, произошедшее в Западной Неваде. Ближайший населенный пункт от эпицентра находился на расстоянии» 59 км. К тому же, вблизи эпицентра не оказалось не только приборов сильных движений, но и регулярных сейсмостанций. Ближайшая с/станция, зафиксировавшая событие, находилась на расстоянии» 39 км. При отсутствии сведений или их крайней малочисленности построение изосейст вблизи эпицентра может быть произведено только теоретическими расчетами. Используются среднемировые или региональные эмпирические зависимости затухания параметров колебаний. При этом закон затухания обычно описывается одной кривой. Точность таких построений невысока. Выделение в волновом поле землетрясения нескольких зон со своими законами затухания и зависимостями параметров колебаний от параметров очага и среды значительно повышает точность расчетов. В статье предлагается методика расчетов ускорений и интенсивностей, основанная на эмпирических данных. **Цель работы** – исследование макросейсмического поля землетрясения Монте Кристо Рэйндж, 15.05.2020 г., M_W = 6,5: оценка пиковых ускорений и интенсивности вблизи очага этого землетрясения. **Методы исследования** – анализ имеющихся данных о землетрясении, разработка кривых затухания применительно к этому сейсмическому событию, расчет пиковых ускорений грунта, продолжительности колебаний и оценка интенсивности. **Результаты работы** – для землетрясения Монте Кристо Рэйндж, 15.05.2020 г., предложены уравнения затухания пиковых ускорений, и оценен сейсмический эффект.

Ключевые слова: сейсмические воздействия, очаг, магнитуда, пиковое ускорение, пиковая скорость, продолжительность колебаний, интенсивность, макросейсмическое поле.

Благодарность: *Данная работа частично финансируется Департаментом науки и технологии правительства Индии, INT/RUS/RFBR/P-335 и Министерством наук о Земле MoES/PO (Seismo)/1 (304)/2016, а также была выполнена по государственному заданию Института физики Земли им. О.Ю. Шмидта РАН и поддержана Российским фондом фундаментальных исследований (грант №18-55-45010). Региональная сейсмическая сеть Невады (NN) ведет наблюдения по всей Неваде и во многих районах Восточной Калифорнии. Она включает в себя около 450 каналов приборов различного типа, регистрирующих сейсмические сигналы в режиме реального времени. Данные сети NN доступны через IRISDMC (IRISData Management Centre). Центр данных о землетрясениях Южной Калифорнии (Southern California Earthquake Data Center, SCEDC), финансируемый Центром землетрясений Южной Калифорнии (Southern*

California Earthquake Center, SCEC) и другими источниками, содержит полные архивы данных сети SCSN/ CISN (Southern California Seismic Network/California Integrated Seismic Network) с 1932 года по настоящее время. Доступ к сети SCSN, управляемой Калифорнийским технологическим институтом и Геологической службой США, осуществлялся через SCEDC. Сейсмограммы, метаданные и другие данные для этого исследования были получены через Центр данных о землетрясениях в Северной Калифорнии (NCEDC), куда они были предоставлены Калифорнийским университетом Беркли.

Для цитирования: Эртелева О. О., Аптикаев Ф. Ф., Редди Картик К. С. К., Чанда С., Сомала С. Н. Землетрясение Монте Кристо Рэйндж, 15 мая 2020 г.: расчетная интенсивность и макросейсмическое поле. *Геология и геофизика Юга России*. 2022. 12 (1): 62–74. DOI: 10.46698/VNC.2022.92.93.005.

Introduction

On 15th May 2020 at 19 h 03 min 27 sec (GMT) (11 h 03 min 27 sec UTC) a relatively strong earthquake occurred in Monte Cristo Range, western Nevada. The source was located about 55 km west-north-west of Tonopah city (sometimes this event named Tonopah earthquake). The coordinates of epicentre are 38.163°N, 117.859°W. It was located between Candeleria fault and Eastern Columbus Salt Marsh fault type of faulting is a combination of normal and strike-slip (fig. 1).

Magnitude of the event is $M_w = 6.5$. For this level $M_w = M_S$. Depth by USGS estimation is $h = 11$ km, but Nevada seismological laboratory evaluated $h = 2.7$ km (https:// earthquake. usgs. gov/earthquakes/eventpage/nn00725272/executive). Maybe, these estimates are corresponding to lower and upper boundaries of rupture surface. At the same time according to [Wells et al., 1994] width of rupture surface is 10.7 km. Therefore, value of $h = 11$ km is used for the further calculations.

Within 12 hours after the main shock 7 aftershocks of magnitude higher than 4.5 were recorded. The very next day there were two aftershocks with $M_w > 4.5$, followed by one each subsequent couple of days. Four days past the main shock, still aftershocks of magnitude higher than 4 are observed (fig. 2). Aftershocks are concentrated in an ellipti-

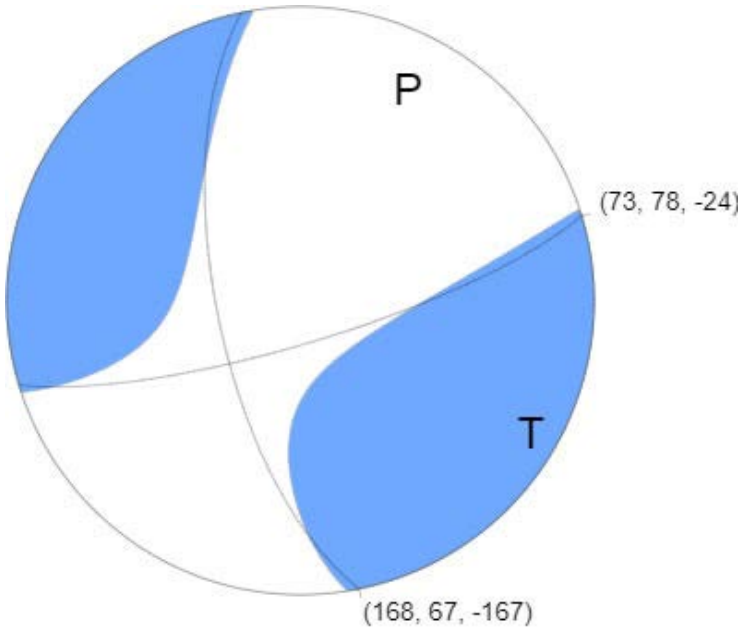

Fig. 1. Moment tensor of Monte Cristo Range earthquake 15.05.2020 (https://earthquake. usgs. gov/earthquakes/eventpage/nn00725272/executive)

Fig. 2. Esmeralda County Sheriff's Office photo of cracks across Highway 95 (http://www. nbmg. unr. edu/Geohazards/Earthquakes/MonteCristoRangeEQ. html)

cal region with major axis roughly oriented NE-SW, except for a few scattered ones SE of the epicentre. There are 2 aftershock zones. One was located at the extending of Candelaria fault; another was at the eastern edge and extended towards Petrified Springs Fault System. The length of mainshock rupture is about 28-35 km long a previously unknown eastward extension of Candelaria fault [Morton et al., 2020; Bormann et al., 2021; Dee et al., 2021; Koehler et al., 2021]. Maximal coseismic slip is 0.8 m [Zheng et al., 2020].

The earthquake occurred in a sparsely populated area, so there were no casualties. But shakings were felt across a large area up to San Francisco, Salt Lake City and Los Angeles. No major damage was reported. This seismic event only damaged U. S. Route 95 between Reno city and Las Vegas: there are cracks (fig. 2).

The purpose of this work

The estimated maximum intensity is VIII (https://earthquake. usgs. gov/earthquakes/eventpage/nn00725272/executive). The nearest seismic station was located at about 39 km. The seismic records and the macroseismic data were absent in the near-field zone. Therefore, it was possible to define the intensity in the far-field only. In proposed research we investigated the seismic effects of the Monte Cristo Range earthquake: we assessed the peak ground accelerations (*PGA*), duration of oscillation (t) and intensity (*I*) in the near-field of this earthquake.

Research methods

In the absence of information or their extremely small number, the construction of isoseists near the epicenter can be made only by theoretical calculations. For this target the global or regional empirical attenuation curves are used. As the rule, the attenuation law is described by single curve. The accuracy of such constructions is low. The separa-

tion of several zones in the earthquake wave field with their individual attenuation laws significantly improves the accuracy of calculations.

For studying the near-field of Monte Cristo Range (Tonopah) earthquake, 15.05.2020, we used the system of *PGA* empirical attenuation curves developed on the basis of the world-wide strong ground motions database [Aptikaev, 2009; Erteleva et al., 2020]. Analyzing the available data on the Monte Cristo Range earthquake, we developed the empirical attenuation curves for this seismic event. Then, for the sites, where the strong ground motions seismic stations were located, *PGA* and t were calculated.

The intensity in the near-field zone were estimated using the *PGA* attenuation equations and correlation relation, which connects *I* at the sites with *PGA*' and t values there.

Table 1

Western Nevada historic significant earthquakes

Year	Date	Time (GMT) h min	Location	Maximal intensity I_{max}	Reference
1868	30.05	0510	Virginia City Area	VII	[Slemmons et al., 1965; Toppozado et al., 1981; 2000; de Polo et al., 2003; 2006]
1869	27.12	0155	Virginia City Area	VIII	[Slemmons et al., 1965; Toppozado et al., 1981; 2000; de Polo et al., 2003; 2006]
1869	27.12	1000	Virginia City Area	VII	[Slemmons et al., 1965; Toppozado et al., 1981; 2000; de Polo et al., 2003; 2006]
1887	03.06	1050	Carson Valley	VIII	[Slemmons et al., 1965; Toppozado et al., 1981; 2000; de Polo et al., 2003; 2006]
1910	21.11	2323	Tonopah Junction	VIII	[Slemmons et al., 1965; Toppozado et al., 2000; de Polo et al., 2006]
1914	18.02	1817	Reno region	VII	[Slemmons et al., 1965; Toppozado et al., 2000; de Polo et al., 2006]
1914	24.04	0834	Reno region	VII	[Slemmons et al., 1965; Toppozado et al., 2000; de Polo et al., 2006]
1915	03.10	0653	Pleasant Valley	VIII-X	[Slemmons et al., 1965; Toppozado et al., 2000; de Polo et al., 2006]
1932	20.12	1010	Cedar Mountain	VIII-X	[Gianella et al., 1934; Slemmons et al., 1965; Toppozado et al., 2000; de Polo et al., 2003; 2006]
1933	25.06	2045	near Wabuska	VII	[Neumann, 1935; Slemmons et al., 1965; Toppozado et al., 2000; de Polo et al., 2006]
1934	30.01	2016	Excelsior Mountains	VIII	[Callaghan et al., 1935; Neumann, 1936; Slemmons et al., 1965; Toppozado et al., 2000; de Polo et al., 2006]
1948	29.12	1253	near Verdi	VII	[Murphy et al., 1951; Slemmons et al., 1965; Toppozado et al., 2000; de Polo et al., 2006]
1954	06.07	1113	Rainbow Mountain	IX	[Murphy et al., 1956; Doser, 1986; Slemmons et al., 1965; Toppozado et al., 2000; de Polo et al., 2003]
1954	24.08	0551	Stillwater Range	IX	[Murphy et al., 1956; Doser, 1986; Slemmons et al., 1965; Toppozado et al, 2000; de Polo et al., 2003]
1954	16.12	1107	Dixie Valley -Fairview Valley	X	[Murphy et al., 1956; Slemmons, 1957; Doser, 1986; Slemmons et al., 1965; Toppozado et al., 2000; de Polo et al., 2003; Caskey et al., 1996; 1997]
2008	21.02	1442	near Wells	VIII	[Smith et al., 2011; de Polo, 2014]

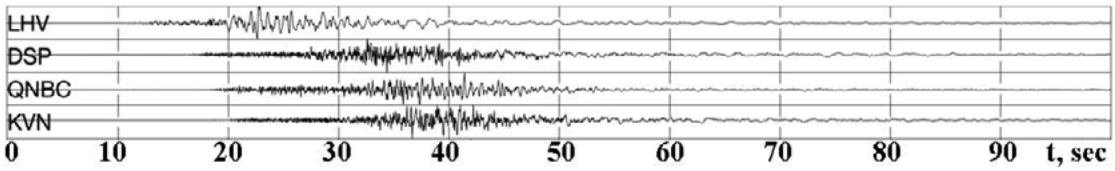

Fig. 3: More intensive accelerograms of Monte Cristo Range (Tonopah) earthquake, E-W horizontal component

The calculated intensities and intensities obtained from strong ground motion records were compared. Using such results, the seismic effect of the Monte Cristo Range earthquake, was estimated.

Tectonics and seismicity of the Monte Cristo Range earthquake region

The region, where source of Monte Cristo Range earthquake, 15.05.2020, is located, is the northeast of the Mina deflection, western Nevada, the central Walker Lane. The Walker Lane is a zone of wide 100-300 km with many active faults [Stewart, 1988; Bennett et al., 2003]. There is complicated tectonics with the thrusts, folds here. A feature of the seismicity of the Walker Lane is the simultaneous existence and interaction of multiple faults with different types of faulting. The strike-slip (left-lateral and right-lateral) and normal faults are characterized for the Mina deflection [Wesnousky, 2012; Lee et al., 2009; Nagorsen-Rinke et al., 2013; Bormann et al., 2016].

Historical seismicity documented in Western Nevada is very reach of the numerous felt and damage seismic events (Table 1). Most earthquakes of this region had a prolonged aftershock process. The same peculiar feature is characteristic of Monte Cristo earthquake.

Strong Motion Data

The Monte Cristo Range (Tonopah) earthquake was recorded by many s/stations. But unfortunately, the epicentral distances were large. We used the accelerograms of 41 stations. The examples of records with maximal *PGA* are shown in fig. 3.

The stations with codes LHV, DSP, QNBC and KVN are within 100 km from epicentre. All these stations are within couple of degrees distance from epicentre with limited coverage in first quadrant. The strong motion data has been corrected for DC shift scaled based on the sensitivity. The closest station to the hypocentre is LHV, which is about 58 km from the epicentre, and the shortest distance from the rupture surface for this station is 35 km. *PGA* value recorded at this station is close to 0.3 m/sec^2 in both the horizontal components, while the THV1 station which is 85 km from the earthquake location recorded *PGA* of 2.18 m/sec^2 along EW direction. This is also the highest *PGA* among all the stations shown in fig. 4, followed by QNBC station recording about 1.5 m/sec^2 on both the horizontal components. All the SCEDC stations had *PGA* within 0.1 to 0.2 m/sec^2. Shaking lasted approximately from 35 sec to 75 sec at the stations considered (fig. 3).

The Fourier amplitude spectra of accelerations for the horizontal and vertical components are also computed. Most of the energy is concentrated around 0.8-2 Hz band. The high frequency decay of these spectra is used to compute kappa factor. Kappa for vertical components hardly has any variation with distance $\kappa = 0.0001R + 0.0320$. The asymptotic

limit as R tends to zero is $\kappa 0 = 0.032$. Kappa for horizontal components is found to follow $\kappa = 0.0059R + 0.0279$ (with $\kappa 0 = 0.0279$).

Empirical attenuation law for Monte Cristo Range earthquake

Because the area near the epicenter of the Monte Cristo Range earthquake is sparsely populated, it is difficult to design shake maps of ground accelerations and isoseists. Therefore, average world empirical dependences of the attenuation of these parameters are used in such cases. There are two intensity maps for this earthquake (https://earthquake. usgs. gov/earthquakes/eventpage/nn00725272/executive): Community Internet Intensity Map (by the USGS DFYI web site) with maximal intensity *MM* VII and Estimated intensity map with maximal intensity *MM* VIII. The accuracy of such constructions is not high. The main reason for the errors is the assumption that the attenuation of seismic effects can be described by a single equation.

It turned out [Aptikaev, 2009; Aptikaev, Erteleva., 2021], that in the engineering range (6-9 points of seismic intensities):

the mean values of accelerations in narrow distance intervals can be approximated by three straight line segments with different attenuations of accelerations and intensities, and different dependencies on earthquake magnitude, focal mechanism, and ground conditions (fig. 4);.

the acceleration attenuation curves for different magnitudes are muted by shifting not along the amplitude axis, but along the distance axis;

in the immediate vicinity of the fault a zone is separated, where the amplitude increase with distance. It was called a fault-field zone in [Aptikaev, Erteleva, 2021];

in the far-field zone the PGA attenuation becomes very dramatically, because the boundary of the near-field and far-field zones is the border of the earthquake source.

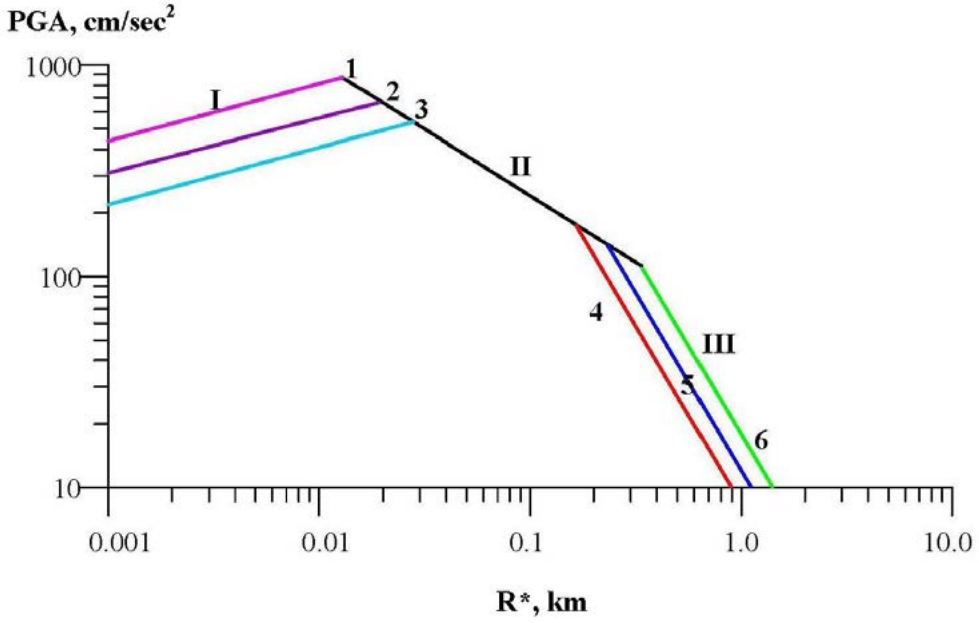

Fig. 4. Attenuation of PGA from empirical data (by Erteleva). Zones: fault-field; II – near-field; III – far-field. Focal mechanism: 1 – thrust; 2 – strike-ship; 3 – normal. Ground category: 4-hard; 5 – intermediate; 6 – soft.

At some distance from the fault, the accelerations depend on magnitude. On the contrary, at the fault surface, many researchers consider acceleration amplitudes to be independent of magnitude [Campbell, 1981; Trifunac, 1976; Bommer et al., 2000; Yamada et al., 2009; Aptikaev, 2009]. Therefore, if we normalize distances according to the law

$$lg\ R^* = lg\ R - 0.33\ M_S, \quad (1)$$

where R is the shortest distance from the fault surface; R^* is the distance normalized by M_S,

then the problem of finding the amplitude attenuation law is greatly simplified, since the magnitude dependence disappears; the accuracy of the estimates is significantly increased: the standard deviation for the worldwide data sample is 0.17 for the fault-field and near – field zones and 0.20 for the far-field zone.

In the fault-field zone, accelerations obey the law:

$$lgPGA\ (R^*) = lgPGA_f + C_f lg\ (1+ R^*) \pm 0.17, \quad (2)$$

where PGA_f is the acceleration at the rupture surface, C_f is a coefficient depending on the focal mechanism (Table 2).

Table 2

Values of PGA_f and coefficient C.

Focal mechanism	PGA_f, cm/sec^2	C_f	PGA_{max}
Thrust	435	52.5	870
Strike-slip	310	38	660
Normal	220	28	535

The maximum values of accelerations are observed at the boundary of the fault-field and near-field zones.

For the Monte Cristo earthquake PGA_f = 260 cm/sec^2. Maximal acceleration PGA_{max} = 590 cm/sec^2 is expected on shortest distance from rupture surface R = 3.2 km. According to model the depth of lower boundary of rupture surface is 11 km, maximal acceleration must be observed on distance about 3 km. For the model of upper boundary of rupture surface is 2.7 km, maximal acceleration must be observed just above rupture surface. For the strong motion stations both models give practically the same results.

For the Monte Cristo earthquake, we have in the fault-field zone

$$lgPGA\ (R^*) = 2.415 + 32.7\ lg\ (1+ R^*) \pm 0.17, \quad (3)$$

In the near-field zone the acceleration amplitudes begin to reduce (see fig. 4), no significant effects of the focal mechanism and ground conditions on the *PGA* amplitude were found. The equation for this zone is:

$$lg\ (PGA,\ cm/sec^2) = 1.75\text{-}0.63\ lg\ R^* \pm 0.15. \quad (4)$$

In the far-field zone, the influence of ground properties on the vibration level is significant: for rock the amplitude level should be reduced and for soft ground to increase. All given estimates refer to the largest amplitude on the horizontal component.

For the far-field zone, an empirical equation is obtained

$$lg\ PGA = C_{gr} - (2.76\text{-}0.17\ M_S)\ lg\ R^* \pm 0.2, \quad (5)$$

where C_{gr} = 0.9 for rock, 1.1 for intermediate ground and 1.3 for soft ground.

For the Monte Cristo earthquake ground conditions are unknown, we are used C_{gr} = 1.1:

$$lg\ PGA = 1.1\text{-}1.655\ lg\ R^* \pm 0.25, \quad (6)$$

There is a sharp increase in the attenuation in the far-field zone. This can only be explained by the fact that the boundary of the near-field and far-field zones is the border of the earthquake source.

Seismic effect of Monte Cristo Range earthquake in the near-field

Rupture length was 28 km [Morton et al., 2020]. The position of the rupture surface is taken as single plane according to the cloud of aftershocks from [Ruhl et al., 2021]. Therefore, our distance estimations are somewhat different from those, given in the publications. The distances were taken by us from the line of the fault.

The seismic effect can be estimated using vibration level value [Aptikaev, 2009; Aptikaev, Erteleva, 2021; Chernov, 2021]. To assess the seismic effect the empirical formulas that describe the relationship between *I* and *PGA* (or *PGV*) value at the observation point [Aptikaev, 2009; Aptikaev, Erteleva, 2021] are used:

$$I = 2.5\ lgPGA + 1.25\ lg\tau + 1.05, \quad (7)$$

$$I = (lg\ PGV + 0.5\ lg\tau_V + 1.8)/0.47, \quad (8)$$

where τ is the duration of oscillation when the acceleration is considered as the ground motion parameter; τ_V is the duration of oscillation when the velocity is considered as the ground motion parameter.

Duration affects the seismic intensity [Aptikaev, 2009; Zaalishvili et al., 2020]. τ is defined as the time interval during which the level of the oscillation envelope exceeds half the maximum value (it was called the pulse width)-[Aptikaev, 2009].

The empirical dependence of the pulse width in the fault-field and near-field zones on the magnitude has the form [Aptikaev, Erteleva, 2021]:

$$lg\tau = 0.33\ M_S - 1.63. \quad (9)$$

The pulse width in these zones does not depend on distance and ground conditions.

In the far-field zone the empirical equation is:

$$lg\tau = 0.17\ M_S + 0.5\ lgR^* + C, \quad (10)$$

where *C* = 0.1 for rock, 0.25 for intermediate ground and 0.65 for soft ground.

Using the strong ground motion records (the velocities records during the main shock of Monte Cristo Range earthquake) [Crowell, 2021], we estimated the duration of velocity oscillations at the locations of the s/stations. Then the observed intensities in these points were calculated by equation (8).

Using the developed attenuation law for Monte Cristo Range earthquake, (see equations (3), (4) and (6)), we computed the intensities expected at the registration sites by equations (7). The corresponding pulse widths were calculated using equations (9) – (10).

At last, to show applicability of the proposed methodology, we compared the computed values of intensities with the values of intensities obtained from strong ground motion records (Table 3). Both values are in good agreement.

Table 3

The recorded and calculated effects of the Monte Cristo Range earthquake, 15.05.2020, intermediate ground

Stations	*R*, km	$PGV_{observed}$	$\tau_{observed}$	$I_{observed}$	$PGA_{calculated}$	$\tau_{calculated}$	$I_{calculated}$
P627	35	4.72	22	6.7	109	5.0	7.0
LHV	43	4.41	19.2	6.6	88	5.5	6.8
P650	52	7.37	25	7.0	65	6.0	6.5
TONO	48	3.41	16.5	6.4	53	5.8	6.3
P132	60	4.15	8.7	6.4	51	6.5	6.3
P649	67	3.44	14.7	6.5	43	6.9	6.2
P133	74	1.85	11,3	5.8	36	7.2	6.0
TVH1	75	2.06	21	5.9	33	7.3	5.9

On the station LHV were recorded velocity and acceleration. To the recorded *PGA* at station LHV and related τ (fig. 3) *I* is 6.2 points. The accuracy of intensity estimations for velocity and acceleration are equal. The differences between estimations are depended on frequency content. Therefore, for station LHV mean value $I = 6.4$ is used.

The standard deviation is 0.3 points only, although all estimates were made without taking into account ground conditions unknown to us.

Now, estimating the *PGA*, τ and corresponding *I* values, we can describe the macroseismic field of the considering seismic event. The intensity above fault is 7.7 points. Then, with distance the intensity is increasing and on distance 3 km it reaches the maximal value $I = 8.6$. Further, the intensity begins to decay and decreases to values of $I = 8.0$ on distance 10 km, $I = 7.0$ on distance 35 km and $I = 6.0$ on distance 73 km.

Discussion of results

Usually, when the classic methodic for assessing intensity by the instrumental data are used, only *PGA* attenuation equation is applied. As a consequence, the resulting evaluations include the great errors, especially for the isoseists close in distance to epicenter.

For the Monte Cristo Range earthquake we obtained $I_0 = 7.7$. Let's note, such value is close to USGS' estimation (https://earthquake. usgs. gov/earthquakes/eventpage/nn00725272/executive).

We are proposing to consider whole earthquake wave field as 3 zones: fault-, near- and far-field ones. Each zone is characterized by the own *PGA* attenuation equation, and dependence on source mechanism and ground conditions. The influence of τ duration is taken into account also. Such approach allows describing a macroseismic field in detailed.

So, using this method, we have obtained that directly near the fault the Monte Cristo Range earthquake intensity can be estimated as 7.7 points. But up to 3 km the intensity value grows and reaches 8.6 point. Then it decreases to the value of $I = 8.0$ on distance 10 km. Isoseists radiuses of the intensity of 7.0 points and 6.0 points are 35 km and 73 km.

Nevertheless, when intensity is estimated, it must be taken into account, that in the far-field zone seismic intensity on the soft grounds increases due to increase in the amplitude and duration of the oscillations. For rock – intensity reduces.

Conclusions

Analysis of available data on the Monte Cristo Range earthquake, 15.05.2020, allowed developing the attenuation curves for this seismic event. They are:

lg*PGA* = 2.415 + 32.7 lg (1+ *R**) ± 0.17 for the fault-field zone,
lg*PGA* = 1.75-0.63 lg *R** ± 0.17. for the near-field zone,
lg*PGA* =1.1-1.655 lg *R** ± 0.25, for the far-field zone.

The peak ground accelerations, durations and intensities were calculated. The intensity above fault is 7.7 points. The maximal intensity *I* = 8.6 is expected on distance 3 km. The intensity of *I* = 8.0, 7.0 and 6.0 points are expected on distances 10 km, 35 km and 73 km correspondingly.

By the classic model the maximal intensity near the fault may be estimated by value 8.0 on average.

As the result, the seismic effect near the Monte Cristo Range earthquake epicenter, 15.05.2020, was estimated in detailed.

Conflict of interest

The authors declare no conflict of interest.

References

1. Aptikaev F. Review of empirical scaling of strong ground motion for seismic hazard analysis. Selected topics in earthquake engineering – from earthquake source to seismic design and hazard mitigation (ed. Mihailo D. Trifunac). International conference on earthquake engineering (2009; Banja Luka). Banja Luka, Republic of Srpska, B&H: N. I. G. D. Nezavisne novine, d. o. o., 2009. pp. 27-54.

2. Aptikaev F., Erteleva O. System of acceleration attenuation equations. Prospects for development of engineering survey in Russian Federation. Materials of the 16th All-Russian Conference of prospecting organizations (Moscow, December 1-3). Moscow. Geomarketing LLC, 2021. pp. 406-411, DOI: 10.25296/978-5-6040982-3-3-2021-12-1-764 (In Russ.)

3. Bennett R.A., Wernicke B.P., Niemi N.A., Friedrich, A. M., Davis J.L. Contemporary strain rates in the northern Basin and Range province from GPS data. Tectonics, 2003. Vol. 22. No. 2. Art №1008. – DOI: 10.1029/2001tc001355

4. Bommer J.J., Martinez-Pereira A. Strong-motion parameters: definition, usefulness and predictability. Proc. XII World Conference on Earthquake Engineering (Auckland, January 1 – February 4, 2000). Auckland, New Zealand, 2000. Paper No. 0206.

5. Bormann, J., Hammond, W. C., Kreemer, C., and Blewitt, G. Accommodation of missing shear strain in the central Walker Lane, western North America – constraints from dense GPS measurements. Earth and Planetary Science Letters, 2016. Vol. 440. pp. 169-177.

6. Bormann J.M., Morton E.A., Smith K.D., Kent G.M., Honjas W.S., Plank G.L., Williams M.C. Nevada Seismological Laboratory rapid seismic monitoring deployment and data availability for the 2020 M6.5 Monte Cristo Range, Nevada earthquake sequence. Seism. Research Letters, 2021. Vol. 92. pp. 810-822.

7. Callaghan E., Gianella V.P. The earthquake of January 30, 1934, at Excelsior Mountains, Nevada. Bull. Seism. Soc. Am., 1935. Vol. 25. pp. 161-168.

8. Campbell K.W. Near-source attenuation of peak horizontal acceleration. Bull. Seism. Soc. Am., 1981. Vol. 71. No. 6. pp. 2039-2070.

9. Caskey S.J., Wesnousky S.G. Static stress changes and earthquake triggering during the 1954 Fairview Peak and Dixie Valley earthquakes, central Nevada. Bull. Seism. Soc. Am., 1997. Vol. 87. No. 3. pp. 521-527.

10. Caskey S.J., Wesnousky S.G., Zhang P., Slemmons D.B. Surface faulting of the 1954 Fairview Peak (MS 7.2) and Dixie Valley (MS 6.8) earthquakes, central Nevada. Bull. Seism. Soc. Am., 1996. Vol. 86. No. 3. pp. 761-787.

11. Chernov Yu. K. The experience of detailed probabilistic assessments of possible seismic effects on the territory of North Ossetia-Alania. Geology and Geophysics of Russian South, 2021. Vol. 11. No. 2. pp. 87-102. DOI: 10.46698/VNC.2021.83.10.007. (in Russ.).

12. Crowell B. D. Near-Field Strong Ground Motions from GPS-Derived Velocities for 2020 Intermountain Western United States Earthquakes. Seism. Research Letters, 2021. Vol. 92. 2A. pp. 840-848. DOI: 10.1785/0220200325

13. Dee S., Koehler R. D., Elliott A. J., Hatem A. E., Pickering A. J., Pierce I., Seitz G. G., Collett C. M., Dawson T. E., De Masi C., de Polo C. M., Hartshorn E. J., Madugo C. M., Trexler C. C., Verdugo D. M., Wesnousky S. G., Zachariasen J. Surface Rupture Map of the 2020 M 6.5 Monte Cristo Range earthquake, Esmeralda and Mineral counties, Nevada.-Nevada Bureau of Mines and Geology, 2021. Map 190, 2 sheets, scale 1:14000. 26 p.

14. De Polo C. M., Ramelli A. R., Hess R. H., Anderson J. G. Re-evaluation of pre-1900 earthquakes in western Nevada, Nevada Bureau of Mines and Geology, 2003. Open-File Rept. 03-3. 175 p.

15. De Polo C. M., Garside T. M. The November 21, 1910 Tonopah Junction earthquake, and the February 18, 1914 and April 24, 1914 Reno earthquakes in Nevada, Nevada Bureau of Mines and Geology, 2006. Open-File Rept. 06-2. 102 p.

16. De Polo C. M. High Probability of Foreshock Occurrence and Significant Probability of Multiple Events Associated with Magnitude 6 Earthquakes in Nevada, U. S. A. Seism. Research Letters, 2014. Vol. 85. No. 3. pp. 601-608. DOI: 10.1785/0220120071

17. Dixon T. H., Miller M., Farina F., Wang H., Johnson D. Present-day motion of the Sierra Nevada block and some tectonic implications for the Basin and Range province, North America Cordillera. Tectonics, 2000. Vol. 19. No. 1. pp. 1-24.

18. Doser D. I. Earthquake processes in the Rainbow Mountain – Fairview Peak – Dixie Valley, Nevada, region 1954-1959. J. Geophysical Research, 1986. Vol. 91. pp. 12,527-12,586.

19. Gianella V. P., Callaghan E. The Cedar Mountain, Nevada, earthquake of December 20, 1932. Bull. Seism. Soc. Am., 1934. Vol. 24. No. 4. pp. 345-384. DOI: 10.1785/BSSA0240040345

20. Koehler R. D., Dee S., Elliott A., Hatem A., Pickering A., Pierce I., Seitz G. Field Response and Surface Rupture Characteristics of the 2020 MM 6.5 Monte Cristo Range Earthquake, Central Walker Lane, Nevada. Seism. Research Letters. January 27, 2021. Vol. 92. pp. 823-839. DOI: 10.1785/0220200371

21. Lee J., Garwood J., Stockli D. F., Gosse J. Quaternary faulting in Queen Valley, California-Nevada: Implications for kinematics of fault-slip transfer in the eastern California shear zone – Walker Lane belt. Geological Soc. Am. Bull., 2009. Vol. 121. No. 3. pp. 599-614. DOI: 10.1130/B26352.1

22. Morton E., Ruhl C. J., Smith K., Bormann J. M., Hatch R. L., Ichinose G. A. The 2020 M6.5 Monte Cristo Range, NV Earthquake and Aftershock Sequence. Poster Presentation No. 057 at 2020 SCEC Annual Meeting, 2020, August.

23. Murphy L., Cloud W. United States earthquakes. 1954. U. S. Coast and Geodetic Survey. Serial No. 793. Washington: United States Government printing office, 1956. 110 p.

24. Murphy L. M., Ulrich F. P. United States earthquakes. 1948. U. S. Coast and Geodetic Survey. Serial No. 746. Washington: United States Government printing office, 1951. 50 p.

25. Nagorsen-Rinke, S., Lee, J., Calvert, A. Pliocene sinistral slip across the Adobe Hills, eastern California-western Nevada – kinematics of fault slip transfer across the Mina deflection. Geosphere, 2013. Vol. 9. No. 1. pp. 37-53.

26. Neumann R. United States earthquakes. 1933. U. S. Coast and Geodetic Survey. Serial No. 579. Washington: United States Government printing office, 1935. 83 p.

27. Neumann R. United States earthquakes. 1934. U. S. Coast and Geodetic Survey. Serial No. 593. Washington: United States Government printing office, 1935. 101 p.

28. Ruhl C. J., Morton, E. A., Bormann, J. M., Hatch-Ibarra, R., Ichinose, G., Smith, K. Complex fault geometry of the 2020 Mww6.5 Monte Cristo Range, Nevada earthquake sequence. Seism. Research Letters, 2021. Vol. 92. No. 3. pp. 1876-1890. DOI: 10.1785/0220200345

29. Slemmons D.B. Geological effects of the Dixie Valley- Fairview Peak, Nevada, earthquakes of December 16, 1954. Bul- letin of the Seismological Society of America, 1957. Vol. 47. No. 4. pp. 353-375.

30. Slemmons D.B., Jones A.E., Gimlett J.I. Catalog of Nevada earthquakes, 1852-1960. Bull. Seismol. Soc. Am., 1965. Vol. 55. pp. 537-583.

31. Smith K., Johnson C., Davies J., Agbaje T., Knezevic S. Antoniijevic, and G. Kent. The 2011 Hawthorne, Nevada Earthquake Sequence; Shallow Normal Faulting. Abstract S53B-2284 presented at 2011 Fall Meeting, AGU, San Francisco, Calif., 5-9 Dec.

32. Stewart J.H. Tectonics of the Walker Lane belt, western Great Basin – Mesozoic and Cenozoic deformation in a shear zone in W.G. Ernst, editor, Metamorphism and crustal evolution of the western United States (Rubey Volume VII): Englewood Cliffs, New Jersey, Prentice-Hall, 1988. pp. 681-713.

33. Toppozada T.R., Real C.R., Parke D.L. Preparation of isoseismal maps and summaries of reported effects for pre – 1900 California earthquakes, Cal. Div. Mines Geol., 1981. Open-File Rept. 81-11SAC. 182 p.

34. Toppozada T., Branum D., Petersen M., Hallstrom C., Cramer C., Reichle M. Epicenters of and areas damaged by M ≥ 5 California earthquakes, 1800-1999, Cal. Div. Mines Geol., 2000. Map Sheet 49, Poster.

35. Trifunac M.D. Preliminary analysis of the peaks strong earthquake ground motion-dependece of peaks on earthquake magnitude, epicentral distance, and recording site conditions. Bull. Seism. Soc. Am., 1976. Vol. 66. No. 1. pp. 189-219.

36. Wells D.L., Coppersmith K.J. New empirical relationships among magnitude, rupture length, rupture width, rupture area, and surface displacement. Bull. Seis. Soc. Am., 1994. Vol. 84. No. 4. pp. 974-1002.

37. Wesnousky S.G., Bormann J.M., Kreemer C., Hammond W.C., Brune J.N. Neotectonics, geodesy, and seismic hazard in the northern Walker Lane of the western North America: Thirty kilometers of crustal shear and no strike-slip? Earth Planet. Sci. Lett., 2012. Vol. 329. pp. 133-140. DOI: 10.1016/j. epsl. 2012.02.018.

38. Yamada M., Olsen A., Heaton T. Statistical features of short- and long-period near-source ground motion. Bull. Seism. Soc. Am., 2009. Vol. 99. No. 6. pp. 3264-3274. DOI: 10.1785/0120090067

39. Zaalishvili V.B., Pinar A., Erdik M., Burdzieva O. G, Melkov D.A. Issues of seismic risk assessment of Vladikavkaz city. Geology and Geophysics of Russian South, 2020. Vol. 10. No. 3. pp. 94-113. DOI: 10.46698/VNC.2020.47.51.006 (in Russ.)

40. Zheng A., Chen X., Xu W. Present day deformation mechanism of the northeastern Mina deflection revealed by the 2020 Mw 6.5 Monte Cristo Range earthquake // Geophysical Research Letters, 2020. Vol. 47. e2020GL090142. DOI: 10.1029/2020GL090142